

A systematic study of the effects of volatile species on the structure and physical properties of amorphous SiO_2

Lindsay M. Harrison¹, Alisha N. Clark¹, Adam R. Sarafian², Jean-Paul Davis³, Steven D. Jacobsen⁴, Joshua P. Townsend³, Craig D. Nie², Lisa A. Moore², Matthew E. McKenzie², James E. Tingley², Galan G. Moore², and Randall E. Youngman²

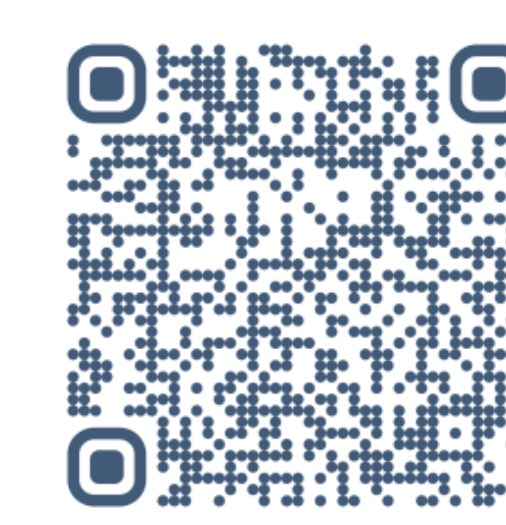
¹ University of Colorado, Boulder; ² Corning, Incorporated; ³ Sandia National Laboratories; ⁴ Northwestern University

1. Introduction

Volatiles lower the solidus and facilitate melting in Earth, the moon, and Mars, which are enriched in OH, F, and Cl, respectively. We aim to understand the atomistic mechanisms that control the volumetric and elastic properties of amorphous silicates, which include melts and glasses, their frozen counterparts. We performed a suite of experiments to constrain the elastic properties of glasses containing OH, F, and Cl (as melt analogues) at ambient pressures and under ramp compression up to 10 GPa. We used resonant ultrasonic spectroscopy and gigahertz ultrasonic interferometry to measure the elastic moduli and wave speeds of volatile-doped silicas at ambient pressure. To probe the properties of these doped silicas at higher temperatures and pressures, we used shockless dynamic compression on the pulsed-power machine Thor and compressed SiO_2 glass samples from 0 to 10 GPa using 10 mm-wide stripline experiment geometry. Shockless ramp compression follows a quasi-isentropic path, which is comparable to the mantle geotherm, so results from these experiments are directly comparable to melts in planetary interiors. We also performed Raman spectroscopy, Fourier transform infrared spectroscopy, magic-angle spinning nuclear magnetic resonance spectroscopy, and molecular dynamics simulations to interpret the differences in elastic behavior between these volatile-doped silicas.

References & acknowledgments

Please scan the QR code for a full list of references.



Sandia National Laboratories is a multimission laboratory managed and operated by National Technology & Engineering Solutions of Sandia, LLC, a wholly owned subsidiary of Honeywell International Inc., for the U.S. Department of Energy's National Nuclear Security Administration under contract DE-NA0003525.

Samples provided by Corning, Incorporated.

This work is supported by the National Science Foundation under Grant EAR-1952641.



5. Conclusions

Key takeaways

- Shear modulus and shear wave speeds show weak dependence on OH content, but F- and Cl-doped silicas show stronger dependence on volatile content.
- Between OH-, F-, and Cl-doped silicas, compressive wave speeds and bulk modulus show similar elastic behavior with respect to increasing dopant concentration and pressure.
- OH-silica and F, Cl doped silicas have distinctly different effects on the silicate network, despite bonding to similar sites and forming terminal bonds.

Future directions

- We plan to obtain compressional wave velocities using GHz interferometry and can calculate 1-atm bulk moduli for the volatile-doped silicas.
- We will take high-precision Raman measurements of OH-doped silicas, to resolve features at low wave numbers.
- Since F and Cl have different effects on the silicate network from OH, it would be interesting to perform shockless ramp compression experiments to investigate high-pressure behavior.

2. Ramp compression

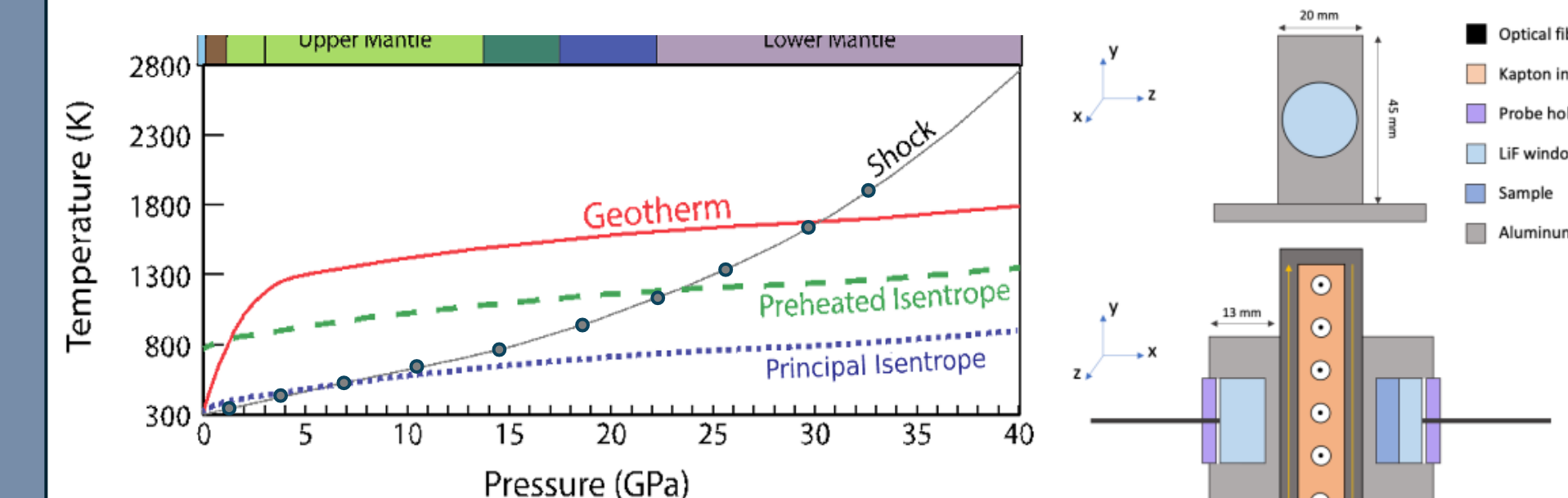


Fig. 1. A) A photo of Thor at the Dynamic Integrated Compression Experimental (DICE) facility at Sandia National Laboratories. The sample is mounted in the center of the circular central power flow section. B) Graph showing different experimental P-T paths with the geotherm for comparison. C) Sample mount schematic: one side consists of a LiF window mounted directly onto the aluminum panel, and the other side consists of a LiF window and SiO_2 glass sample mounted onto the aluminum panel. Current flows along the direction of the yellow arrows.

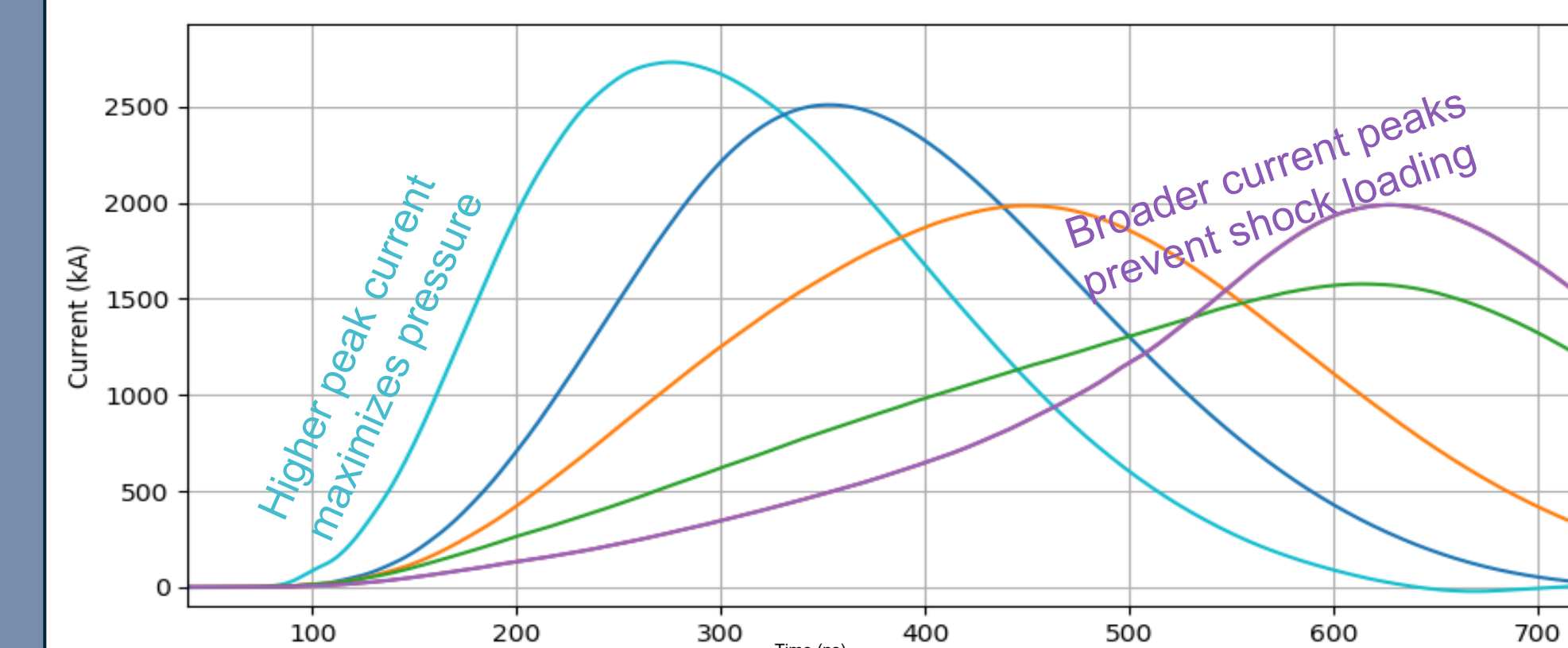


Fig. 2. Examples of pulse shapes: offsets of trigger timings control distribution of current over time. The application of current over a span of time changes the peak current of each shot. Peak current, sample material, and stripline width control peak pressures of the experiment. Each shot is uniquely tailored to achieve desired experimental pressures without shocking the sample.

3. Results/physical properties from Thor

- Particle velocities at the sample-window interface were measured using VISAR and PDV.
- Velocity waveforms are obtained by applying refractive index corrections.
- After applying refractive index corrections, the drive-side and sample-side velocity waveforms are used as inputs for inverse Lagrangian analysis (ILA).
- ILA maps the measured velocity of window + sample to the in-material velocity, that is also self-consistent with LiF window velocity waveform to obtain Lagrangian sound velocity, density, and longitudinal stress.¹

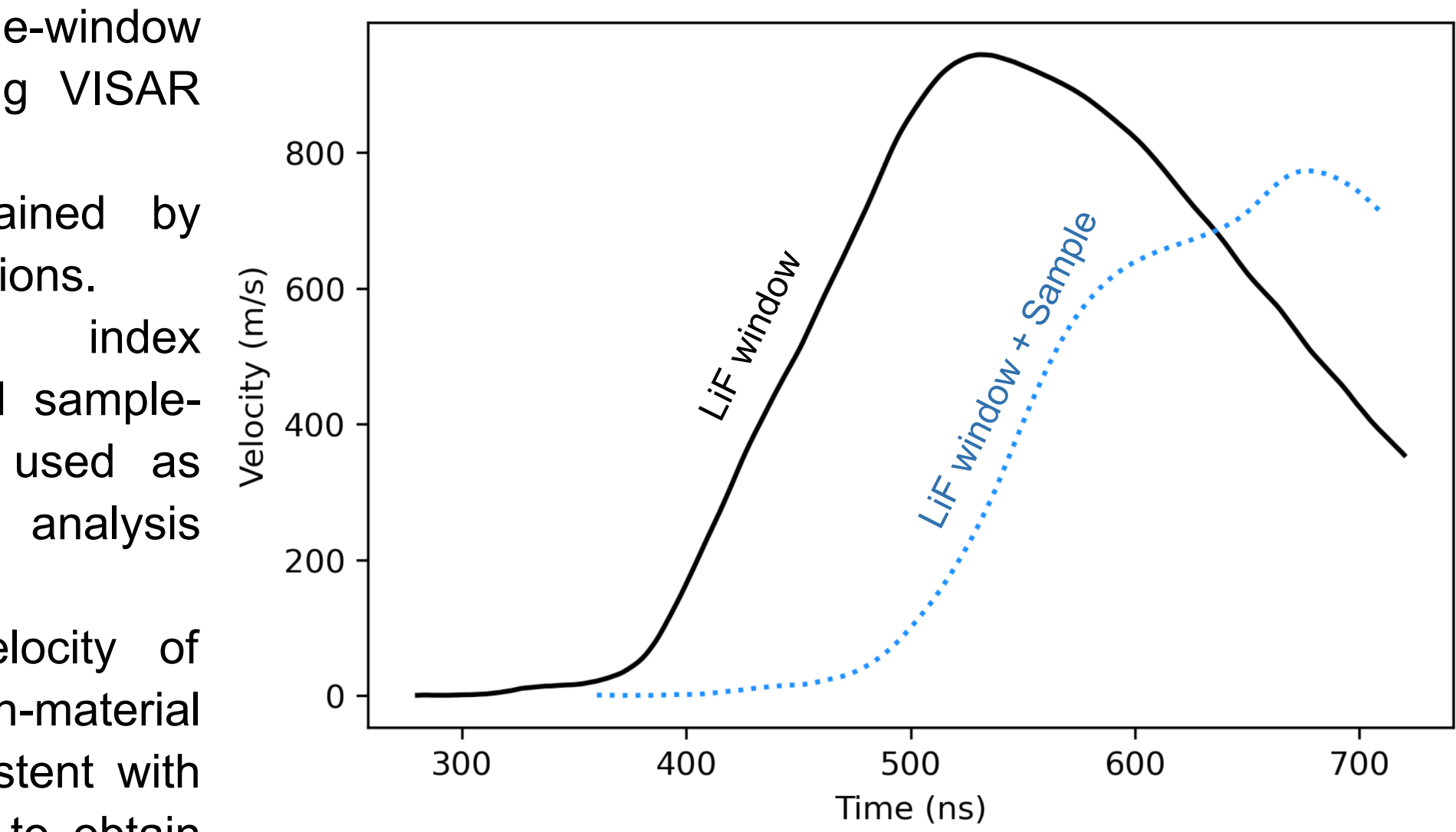
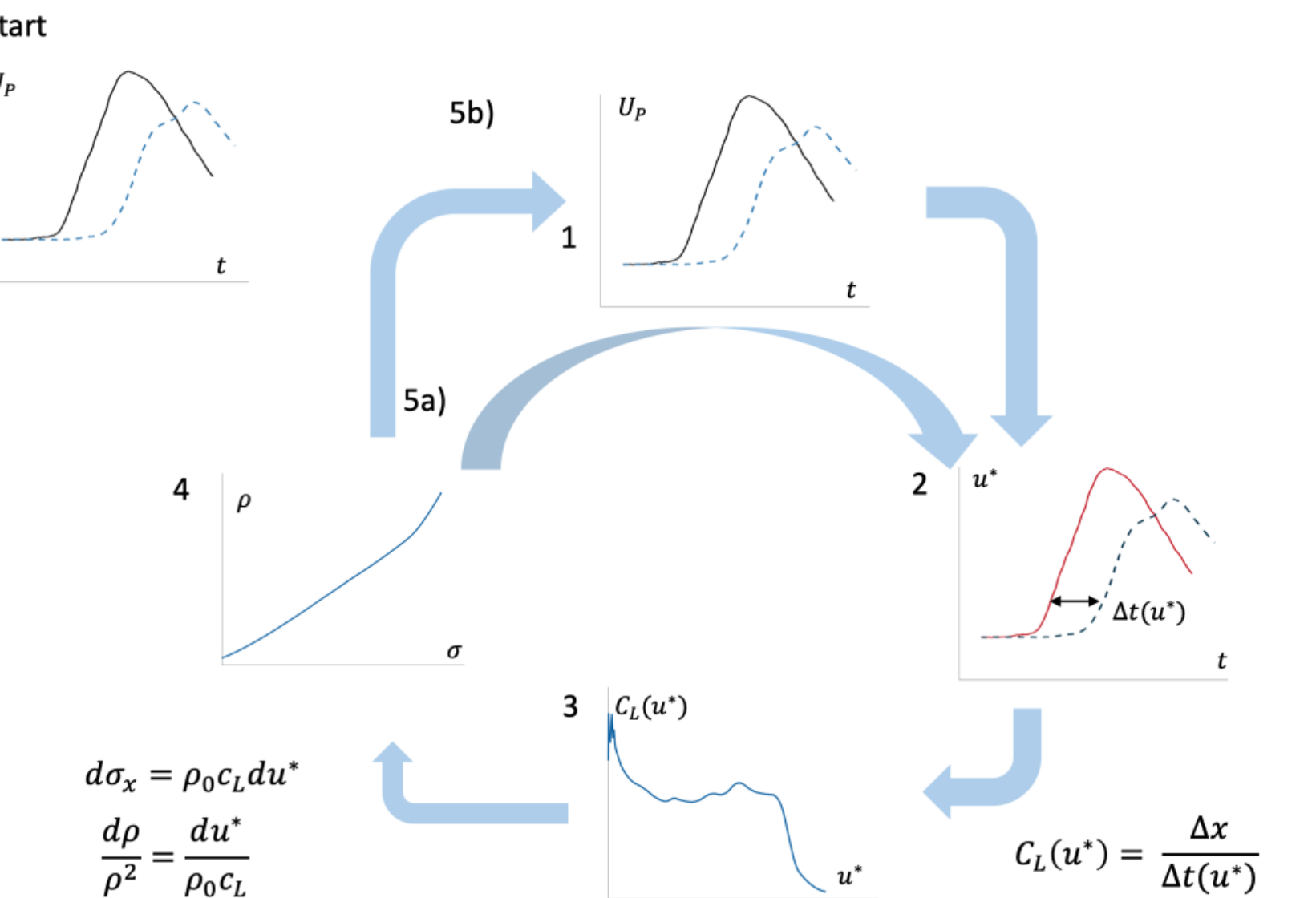
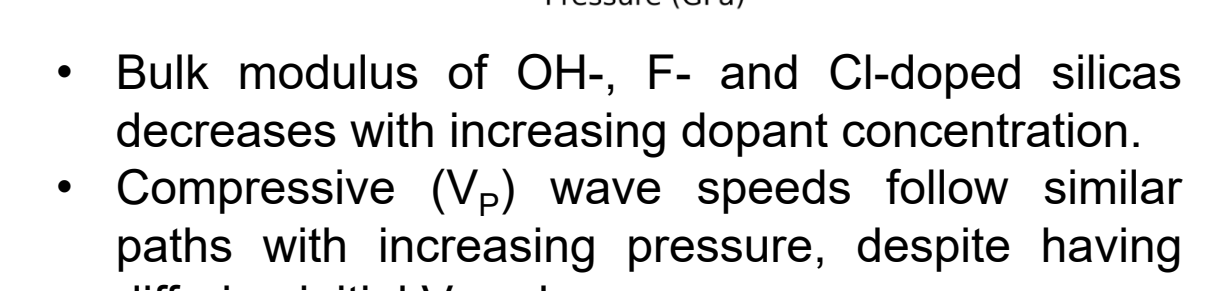
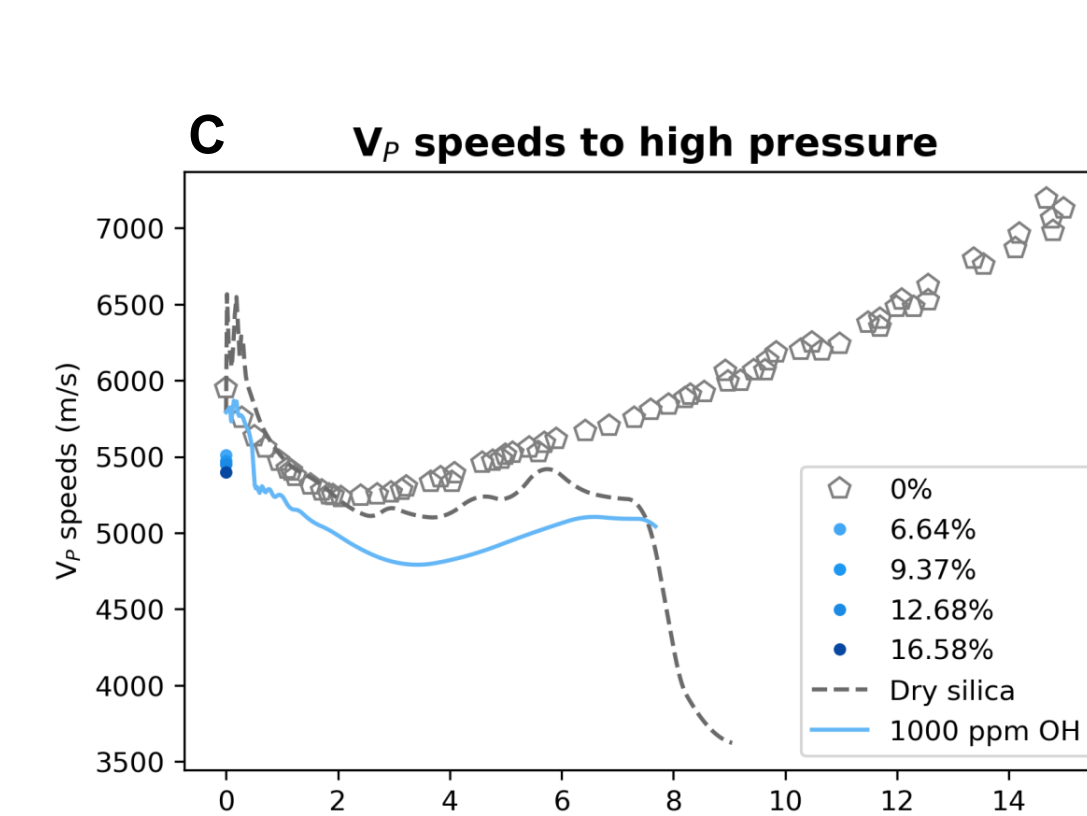
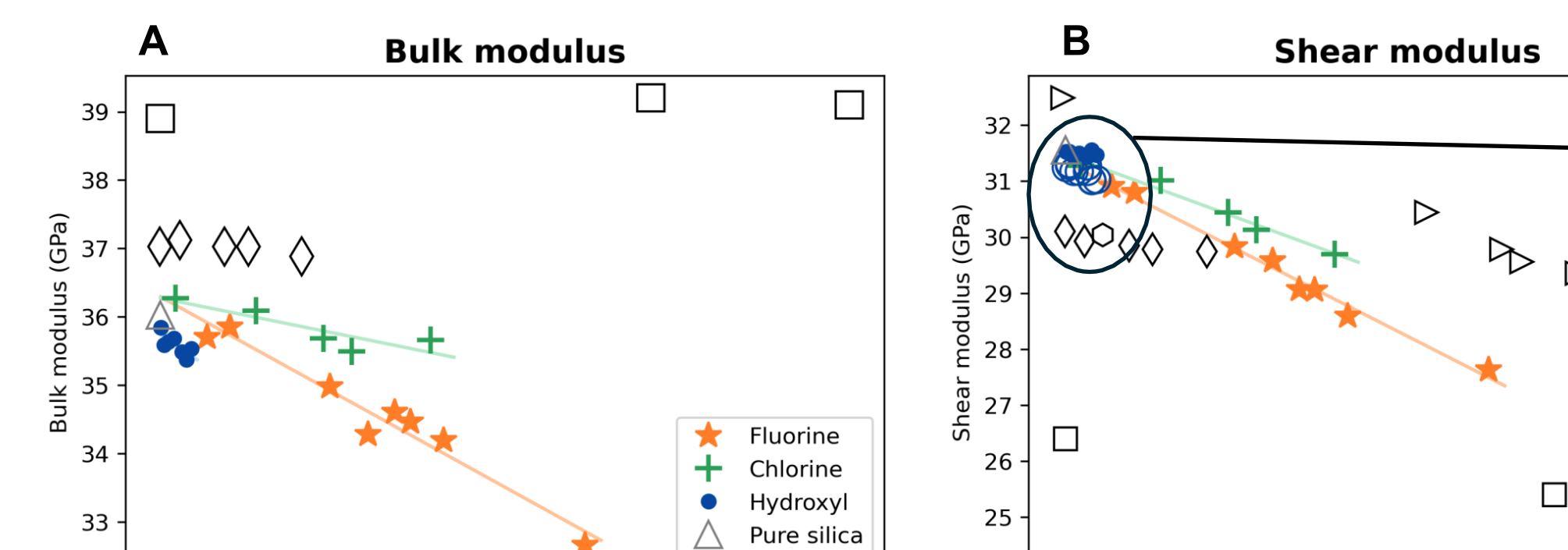


Fig. 3. Left, a plot showing the true velocity waveforms of the drive side (LiF window) and the sample side (window and sample). These waveforms are used as inputs for inverse Lagrangian analysis, described in the flowchart at above right.



4. Insights from 1-atm elastic and structural studies



• Bulk modulus of OH-, F- and Cl-doped silicas decreases with increasing dopant concentration.

• Compressive (V_P) wave speeds follow similar paths with increasing pressure, despite having differing initial V_P values.

• Shear modulus of F- and Cl-doped silicas decreases with concentration, but changes very little in OH-doped silicas up to 0.5 mol%.

• Shear (V_S) wave speeds of OH-doped

silicas increase with pressure, while shear moduli

of F- and Cl-doped silicas decrease with pressure.

Fig. 4. A) Bulk modulus of several doped silicas. B) Shear modulus showing a closer look at shear moduli for OH-doped silicas at lower concentrations. Shear moduli measured from GHz interferometry is represented by hollow blue circles. C) V_P (longitudinal) wave speeds. D) V_S (shear) wave speeds. E) Compression curve of several OH-containing silicas.² Other data: Squares – OH-containing rhyolite from Liu et al. (2023) (3); Diamonds – CO_2 -doped silica from Seifert et al. (2011) (4); Circles – OH-containing haplogranite glass from Malfait et al. (2011) (5); Pentagons – silica glass from Weigel et al. (2019) (6)

Molecular dynamics simulations

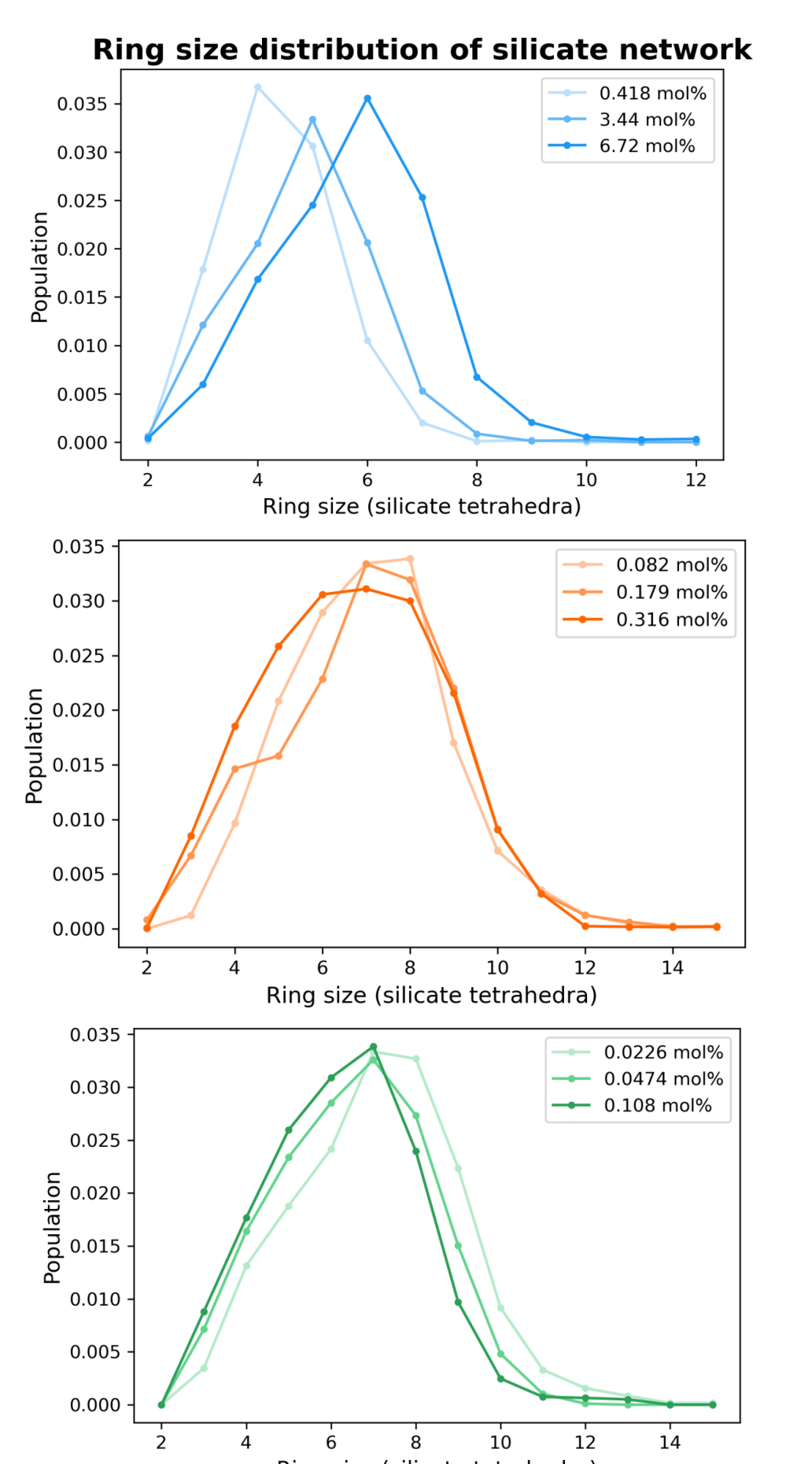


Fig. 5. Silicate tetrahedra ring size distribution across doped silicas. A) OH-doped silicas; B) F-doped silicas; C) Cl-doped silicas. With increasing concentration, OH-doped silicas show increases in larger ring populations, whereas F- and Cl-doped silicas show increases in smaller ring populations.

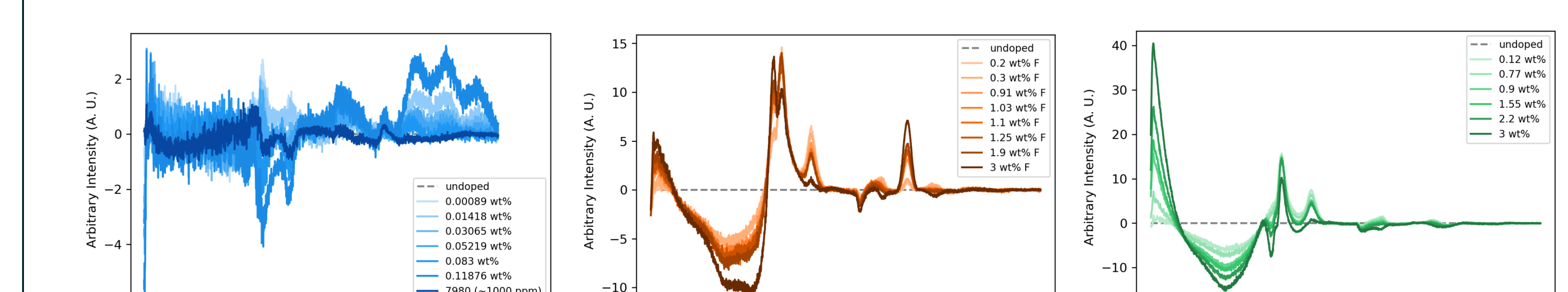


Fig. 6. Raman difference spectra plots of several doped silicas: A) OH-doped silicas; B) F-doped silicas; C) Cl-doped silicas. The saturation of the hue indicates its relative concentration; lightest colors indicate smaller volatile concentrations, and darker colors indicate larger volatile concentration. Dotted line indicates the difference spectra of undoped (pure) silica.

Raman spectra

- Hydroxyl (blue) shows little change between 200-600 cm^{-1} , which includes peaks that correspond to 5+, 4, and 3-membered rings.
- Fluorine (orange) shows decreasing intensity in peaks attributed to larger (5+) membered rings, as does chlorine (green).
- This difference in spectra may explain the different behavior in elastic properties with respect to concentration.